magnetochemistry

MDPI

Article

Large Perpendicular Exchange Energy in Tb_xCo_{100-x}/Cu(t)/$[Co/Pt]_2$ Heterostructures

Sina Ranjbar *, Satoshi Sumi, Kenji Tanabe and Hiroyuki Awano

Toyota Technological Institute, Nagoya 468-8511, Japan; sumi@toyota-ti.ac.jp (S.S.); tanabe@toyota-ti.ac.jp (K.T.); awano@toyota-ti.ac.jp (H.A.)

* Correspondence: sina.ranjbar@toyota-ti.ac.jp

Abstract: In order to realize a perpendicular exchange bias for applications, a robust and tunable exchange bias is required for spintronic applications. Here, we show the perpendicular exchange energy (PEE) in the Tb_xCo_{100-x}/Cu/$[Co/Pt]_2$ heterostructures. The structure consists of amorphous ferrimagnetic Tb–Co alloy films and ferromagnetic Co/Pt multilayers. The dependence of the PEE on the interlayer thickness of Cu and the composition of Tb–Co were analyzed. We demonstrate that the PEE can be controlled by changing the Cu interlayer thickness of $0.2 < t_{Cu} < 0.3$ (nm). We found that PEE reaches a maximum value ($\sigma_{Pw} = 1$ erg/cm^2) at around x = 24%. We, therefore, realize the mechanism of PEE in the Tb_xCo_{100-x}/Cu/$[Co/Pt]_2$ heterostructures. We observe two competing mechanisms—one leading to an increase and the other to a decrease—which corresponds to the effect of Tb content on saturation magnetization and the coercivity of heterostructures. Sequentially, our findings show possibilities for both pinned layers in spintronics and memory device applications by producing large PEE and controlled PEE by Cu thickness, based on Tb_xCo_{100-x}/Cu/$[Co/Pt]_2$ heterostructures.

Keywords: perpendicular magnetic anisotropy; ferrimagnet; perpendicular exchange bias; amorphous thin films; spintronic applications

Citation: Ranjbar, S.; Sumi, S.; Tanabe, K.; Awano, H. Large Perpendicular Exchange Energy in Tb_xCo_{100-x}/Cu(t)/$[Co/Pt]_2$ Heterostructures. *Magnetochemistry* **2021**, *7*, 141. https://doi.org/10.3390/magnetochemistry7110141

Academic Editor: Atsufumi Hirohata

Received: 28 September 2021
Accepted: 20 October 2021
Published: 25 October 2021

1. Introduction

The exchange bias (EB) phenomenon was discovered more than half a century ago by Meiklejohn and Bean [1]. EB can be observed through the exchange coupling between ferromagnet (FM)/antiferromagnetic (AFM) layers at the interface [2,3]. Utilizing a large perpendicular EB field as pinned layers in giant-magnetoresistive (GMR) devices, hard-disk drives (HDDs), magnetic random-access memory (MRAM) technologies, and magnetic tunnel junctions (MTJs) have been the subjects of intense attraction because of their potential in spintronic applications [4–9]. On the other hand, in memory device applications, controlling the perpendicular exchange energy (PEE) is a crucial factor [10–13].

The exchange anisotropy energy is generally revealed by the exchange energy, σ_{Pw}, which is the stabilizing energy per unit area of the FM/AFM or ferrimagnet (FIM)/FM interfaces, $H_{ex} = \frac{J_k}{M_s t} = \frac{\sigma_{Pw}}{2M_s t}$, where M_s and t_{FM} are the saturation magnetization and thickness of the FM layer, respectively [14,15]. However, typical AFM/FM systems indicate a limitation in attaining large EB fields (usually below 1 KOe) [16–18], which correlates to challenges in fabricating fine AFM crystals, controlling the AFM domain state, and uncompensated spin moments at the interface [16,17,19]. Thus, it seems that these cannot provide the reasonable necessities for future spintronic applications. Aside from FM/AFM systems, exchange bias also exists in ferrimagnet FIM/FIM [20] and the ferromagnet FIM/FM bilayer [21]. Amorphous rare earth-transition metal (RE-TM) multilayers exhibit strong perpendicular magnetic anisotropy (PMA) and robust coupling interactions at the interface [22,23].

In amorphous ferrimagnetic (FI) rare earth-transition metal (RE-TM) alloy films, there are two kinds of pair interactions, the antiparallel exchange between the RE-TM moments and the parallel exchange of the TM moments themselves; both interactions can provide a

sufficiently strong interlayer coupling with the adjacent FM layer, and can hence provide a higher EB field—even for fully compensated interfaces [24,25].

Few kinds of research regarding the FIM/FIM, FM/FIM composite structures have been performed. Due to their potential for spintronic applications, more investigation is required to understand the mechanisms of these systems [20,26,27].

In this paper, we investigate the perpendicular exchange energy (PEE) between Tb–Co alloy films and Co/Pt multilayers by varying the Tb content of the Tb–Co layer. We observe that both EB and PEE can be tuned by introducing a Cu spacer layer. The PEE attains its maximum σ_{Pw} = 1 erg/cm^2 at x = 24. We also describe the reason for high PEE at x = 24 in the $Tb_xCo_{100-x}(20)/Cu(t)/[Co(0.4)/Pt(2)]_2$ heterostructures. Our findings prove that $Tb_xCo_{100-x}(20)/Cu(t)/[Co(0.4)/Pt(2)]_2$ heterostructures are efficient for spintronic applications, and they have advantages for manipulation by adjusting the Tb concentration.

2. Experimental Method

Figure 1a shows a schematic illustration of our SiO_2/Pt(5)/$Tb_xCo_{100-x}(20)$/Cu(t)/$[Co(0.4)/Pt(2)]_2$ (thicknesses in nm) ($20 < x < 41$) samples, where the numbers in parentheses indicate the thickness in nanometers. The samples are deposited, using an ultrahigh-vacuum magnetron-sputtering system, onto a silicon substrate at room temperature. Co/Pt multilayers were sputtered, through dc sputtering, using two separate targets of platinum and cobalt at an argon-gas pressure level of 0.2 pascal. Tb_xCo_{100-x} films were prepared through co-sputtering using two separate targets of terbium and cobalt. The sample holder rotates during the deposition to ensure a uniform film composition. The thickness of the Tb_xCo_{100-x} layer is fixed at 20 nm. The composition of the films was measured using energy-dispersive X-ray analysis (EDX). The magnetic properties were measured at room temperature using the polar-magneto-optical Kerr effect (PMOKE) and a vibrating sample magnetometer (VSM).

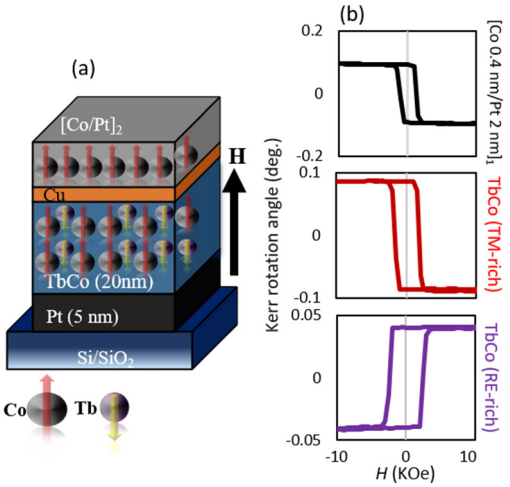

Figure 1. (**a**) Schematic view of the sample layer structure; (**b**) out-of-plane magneto-optic Kerr effect.

3. Results and Discussion

We first determined the magnetic properties of $Tb_xCo_{100-x}(20)/Cu(0.2)/[Co(0.4)/Pt(2)]_2$ systems. Figure 1b shows the hysteresis loops were measured using the polar-magneto-optical Kerr effect (PMOKE) at room temperature for three single-layer samples, a $[Co/Pt]_2$ multilayer film, and Tb–Co films. All samples show the easy axis perpendicular to the film plane. The polarity of the Kerr rotation (θ_K) signals switches, which is consistent with a transition from being Co dominated to being Tb dominated in the magnetic moment.

(MOKE) signal for a single layer of [Co/Pt] and Tb–Co. The MOKE measurement wavelength is 690 nm for visible light. At 690 nm, only the magneto-optical Kerr effect of Co can be measured. This magneto-optical hysteresis of Co shows negative polarity, as shown in Co/Pt in Figure 1b. Similarly, in the TM-rich Tb–Co single-layer sample in

Figure 1b, since the Co in the Tb–Co layer is aligned in the magnetic field direction, the polarity of the hysteresis is negative, as in Co/Pt. On the other hand, in the RE-rich Tb–Co single-layer sample in Figure 1b, the polarity of hysteresis is negative because the Co is aligned in the opposite direction to the magnetic field.

Figure 2a shows the out-of-plane magnetic hysteresis loops were measured using the VSM at room temperature for $Tb_xCo_{100-x}(20)/Cu(0.2)/[Co(0.4)/Pt(2)]_2$ systems with different Tb concentrations. Here, we used the VSM to find the saturation magnetization of the sample, which is summarized in Figure 2b. Figure 2a shows a two-step switching loop, where the first and second loop switches at the low and high magnetic fields correspond to the Tb–Co and [Co/Pt] multilayers, respectively.

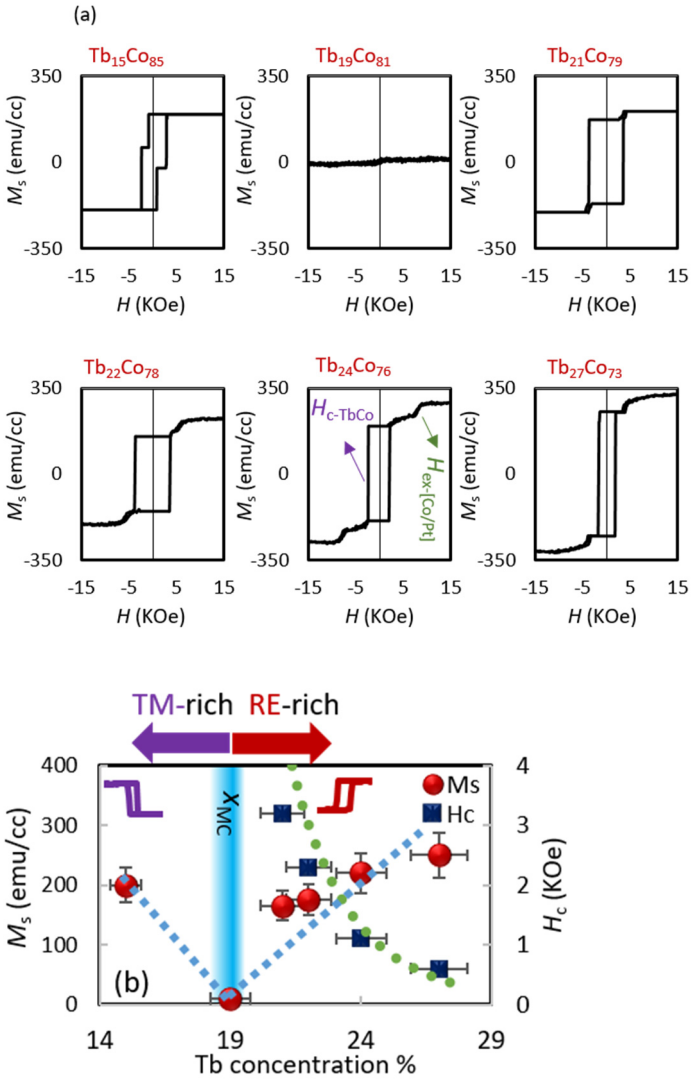

Figure 2. (**a**) The out-of-plane M–H loop for $Tb_xCo_{100-x}/Cu(0.2)/[Co(0.4)/Pt(2)]_2$ heterostructures, and (**b**) M_s and H_c as a function of Tb concentration.

Figure 2b shows the coercive fields (H_c) and the saturation magnetizations (M_s) of $Tb_xCo_{100-x}(20)/Cu(0.2)/[Co(0.4)/Pt(2)]_2$ films at different compositions. From the magnetization curve of the $SiO_2/Pt(5)/Tb_xCo_{100-x}(20)/Cu(0.2)/[Co(0.4)/Pt(2)]_2$ heterostructures, it is seen that the saturation magnetization the M_s of Tb_xCo_{100-x} reaches its magnetization compensation composition point at x_C~19. While the M_s is at its minimum, the coercive fields reach their maximum at the magnetic compensation composition [28–31]. On

the other hand, the perpendicular magnetic anisotropy (K_u) can be calculated using the following equation:

$$K_u \approx \alpha M_s H_c \quad (1)$$

where the α is constant for all samples, since all heterostructures are prepared under the same conditions. By increasing the Tb concentration the K_u value decreases for all samples, which is in good agreement with the previous report [26,32,33].

To realize the insertion layer effect on H_{ex} and the σ_{Pw}, Figure 3a shows the out-of-plane minor loops (+15 KOe = ⇒ 0 Oe = ⇒ + 15 KOe) for the $Tb_{21}Co_{79}/Cu(t_{Cu})/[Co(0.4)/Pt(2)]_2$ heterostructures ($0.2 < t_{Cu} < 1$ nm). This hysteresis loop is shifted away from the zero-field axis to $H = +H_{ex}$, and the width of the loop is 2 H_c, where H_c is the coercive field of a $[Co/Pt]_2$ layer. The hysteresis curve on the high magnetic field side, shown in Figure 2, shows the magnetization reversal of the Co/Pt layer, as evidenced by the negative polarity of the minor loop, as shown in Figure 3a. If this was the result of RE-rich Tb–Co, the polarity would be positive.

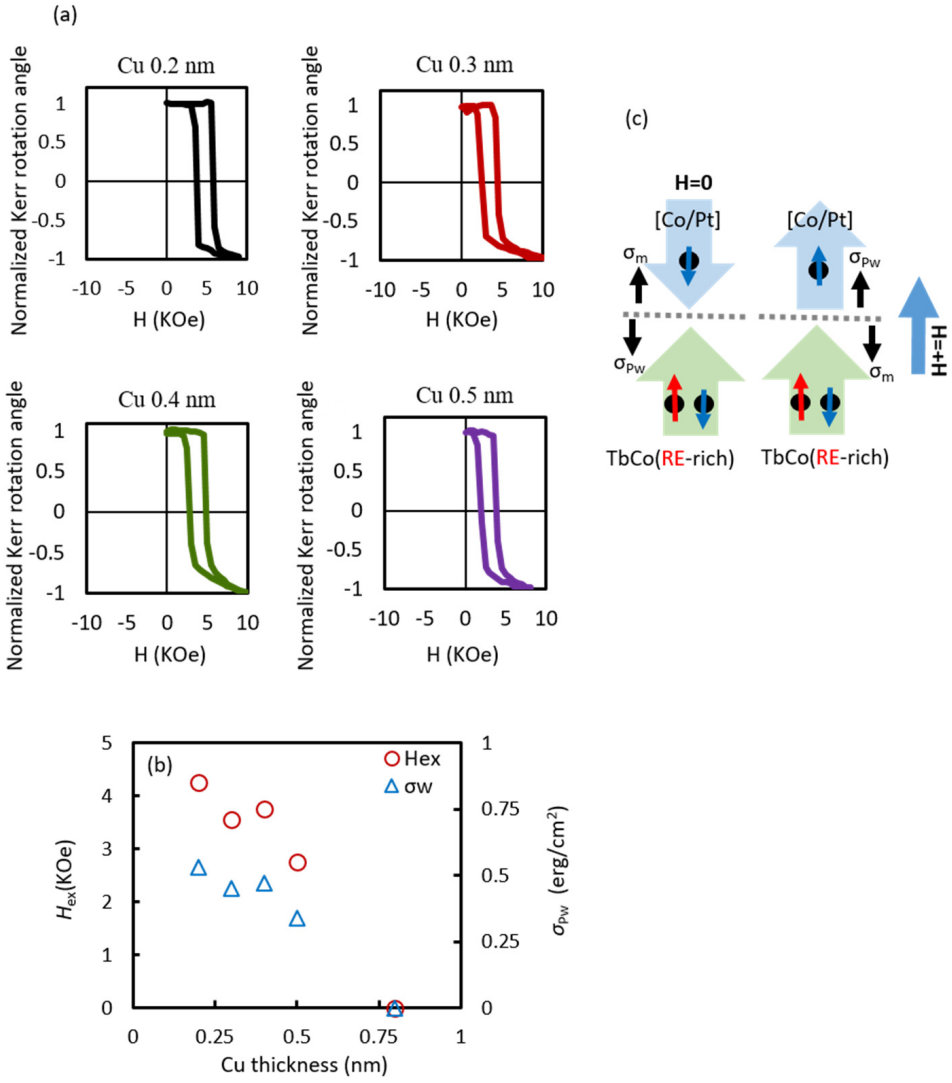

Figure 3. (**a**) Minor loops of the $Tb_{21}Co_{79}/Cu(t_{Cu})/[Co(0.4)/Pt(2)]_2$ heterostructures with various insertion layer thickness; (**b**) changes in the unidirectional anisotropy constant, σ_{Pw}, and exchange anisotropy, H_{ex}, as a function of Cu thickness; (**c**) schematic illustration of the magnetic configuration at the interface of the $Tb_xCo_{100-x}/Cu(0.2)/[Co(0.4)/Pt(2)]_2$ heterostructures.

The Cu interlayer, with a thickness of t_{Cu} = 0.2–1 nm, was employed to tune the perpendicular exchange energy (PEE), σ_{Pw}. The optimization of the insertion layer thickness is necessary to control the PEE value because the removal of the Cu layer causes the exchange coupling to become very large; therefore, it is impractical for the observation of the shift of the hysteresis loop. Ideally, the effect of the Cu insertion causes the intermixing of Tb–Co–Co/Pt that appears during the sputtering process to decrease. Hence, inserting thin Cu layers allows for the improvement of the interface, thus enhancing the effective anisotropy of the stack [34]. Figure 3b shows that by increasing the t_{Cu} over 0.5 nm, the H_{ex} and PEE σ_{Pw} monotonically decrease, which is in agreement with previous reports [35,36]; thus, the optimum H_{ex} and σ_{Pw} values were 4.25 kOe and 0.54 erg/cm^2 at t_{Cu} = 0.2 nm, respectively. As a result, it is clearly demonstrated that the PEE can be controlled by Cu thickness, which indicates additional suitability for memory device applications [10,11].

Figure 3c shows a schematic illustration of the magnetic configuration at the interface of the Tb_xCo_{100-x}/Cu(0.2)/$[Co(0.4)/Pt(2)]_2$ heterostructures. As shown by the zero magnetic field in the model diagram, the magnetization of the Co/Pt layer and the net magnetization of the Tb–Co layer are opposite from one another; therefore, the static magnetic energy at the interface increases. However, since the Co in the Co/Pt layer and the Co in the Tb–Co layer are both oriented in the same direction, the interfacial domain wall energy is low. On the other hand, in the high magnetic field in the model diagram, the static magnetic energy at the interface decreases because the Co/Pt layer is inverted, and conversely, the interfacial domain wall energy increases. In general, when the Co/Pt layer and the Tb–Co layer are directly heterojunctioned, the interfacial domain wall energy is overwhelmingly larger than the interfacial static magnetic energy; thus, it can only be used only for a large exchange bias application. However, it was found that by inserting a small amount of Cu at these interfaces, the interfacial domain wall energy can be controlled and reduced to the desired value. As a result, it can be applied to memory applications that also utilize interfacial static magnetic energy.

To define the EB for each of the heterostructures, the out-of-plane minor loops were measured as shown in Figure 4a. Figure 4b summarized σ_{Pw} and the magnitude of the H_{ex} field, respectively, as a function of the Tb content in the Tb_xCo_{100-x}/Cu(0.2)/$[Co(0.4)/Pt(2)]_2$ heterostructures at room temperature. Between 23 and 25 at.% Tb, the PEE seems to reach its maximal value; toward lower and higher amounts of Tb, some reduction appears. In the first region, both the H_{ex} and σ_{Pw} values increase when the Tb is among 19 < x < 24 atomic percent. Contrarily, in the second region—by increasing the Tb content from x = 24 [31]—both the H_{ex} and σ_{Pw} values decrease and become zero at around x = 30.

In previous studies, it was reported that the EB field reaches its maximum at the compensation point since the compensated sublattices of the FIM film hold no frustrated bonds at the interface to the FM layer [25,37]. However, this behavior cannot be explained directly in our system.

Firstly, this behavior can be explained by taking into account the variation in the exchange energies of the Co–Co pair with changing RE content [38]. Accordingly, the exchange coupling between the Co–Co pairs is the strongest when compared to other pairings ($J_{Co\text{-}Co} > J_{Co\text{-}Tb} > J_{Co\text{-}Pt}$). The $J_{Co\text{-}Co}$ is present at the interface between Tb–Co and [Co/Pt]; therefore, a maximum PEE appears at a lower Tb concentration. Increasing the Tb concentration can decrease the number of Co atoms at the interface, and occasionally it can cause the reduction in the exchange coupling between Co–Co pairs at the interface [21,39].

Moreover, by increasing the Tb content, H_c decreases while M_s increases, which is shown in Figure 2b. Therefore, the variation in the σ_{Pw} value in the reduction in H_c is likely connected with a smaller perpendicular exchange energy, σ_{Pw}, in the ferrimagnet, which should result in smaller perpendicular exchange energy.

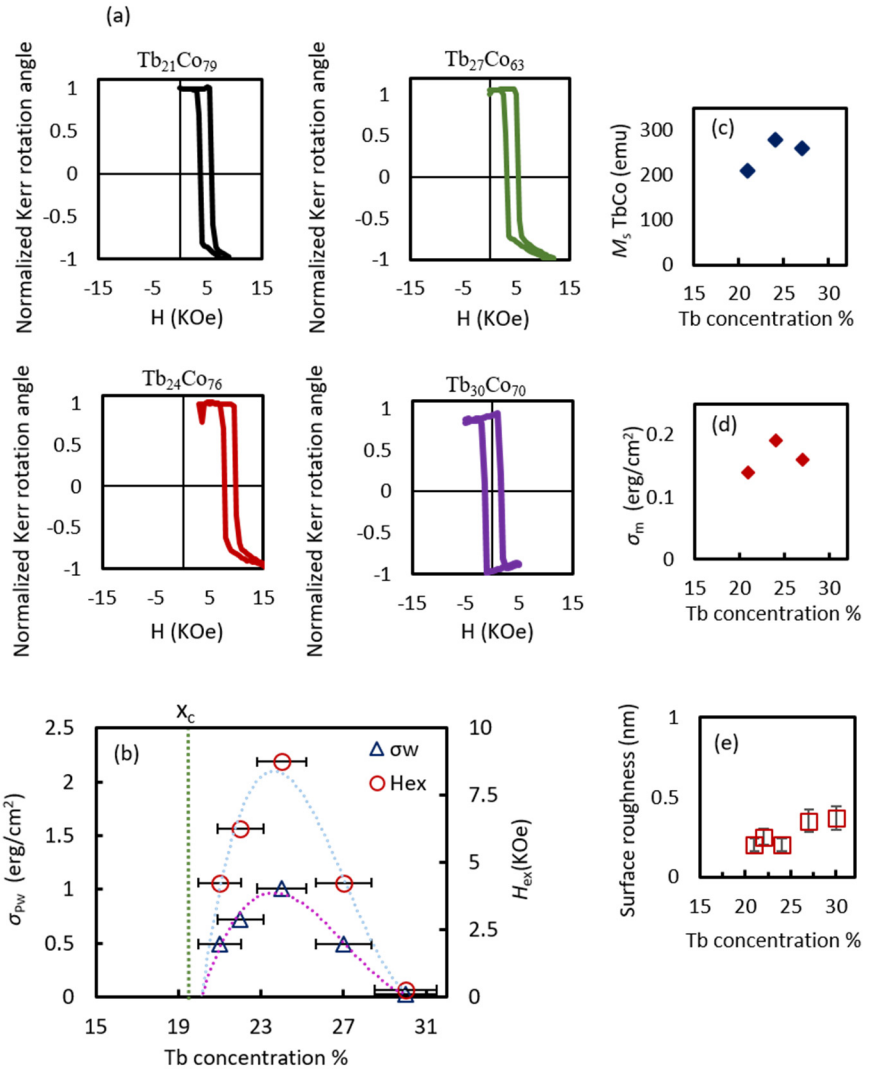

Figure 4. (**a**) Minor loops of the Tb_xCo_{100-x}/Cu(0.2)/[Co(0.4)/Pt(2)]$_2$ heterostructures; (**b**) changes in perpendicular exchange energy, σ_{Pw}, and exchange anisotropy, H_{ex}, as a function of Tb composition; (**c**) Tb–Co magnetization as a function of the Tb content; (**d**) change in magnetostatic energy as a function of Tb composition; (**e**) surface roughness plotted as a function of Tb concentration.

To clarify the variation in σ_{Pw}, the exchange energy can be calculated by the relation in Equation (2). Hence, the total magnetic energy at the interface can be explained by the following equation:

$$E = \sigma_{Pw} + \sigma_m \quad (2)$$

Here, $\sigma_{Pw} = \sigma_{iw} + \sigma_A$, where the first term is the interfacial domain wall energy generated between the Co/Pt layer and the Tb–Co layer; the second term, σ_m, is the static magnetic energy generated between the Co/Pt layer and the Tb–Co layer; and the third term, σ_A, is the magnetic anisotropy generated between the Co/Pt layer and the Tb–Co layer. The interfacial domain wall energy obtained from the inverting magnetic field H_{EX} of the Co/Pt layer is σ_{Pw}.

The anisotropic energy is very small because the Cu intermediate layer greatly attenuates the exchange force between the Co/Pt layer and the Tb–Co layer. Therefore, this σA term can be negligible [40]. To realize the mechanism of the PEE at the interface, we extracted the magnetization information of the samples in Table 1 and summarized them in Figure 4c.

Table 1. Summarized magnetic properties of Tb–Co/$[Co/Pt]_2$ multilayers.

FIM Composition	Ms-Tb–Co (emu/cm^3)	Ms-[Co/Pt] (emu/cm^3)
Tb21Co79	210	1580
Tb24Co76	280	1430
Tb27Co73	260	1550

Figure 4d shows the magnetostatic energy of the Tb_xCo_{100-x}. It is seen that the magnetostatic energy shows the same curvature, which is in good agreement with Figure 4c. Furthermore, the value of magnetostatic energy is considerable and plays an important role in this system [41].

Since EB is an interfacial phenomenon, the surface roughness may affect the magnitude of the exchange bias [19,42,43]. Hence, the effect of the Tb content on the surface morphology of Tb_xCo_{100-x}/Cu(0.2)/$[Co(0.4)/Pt(2)]_2$ heterostructures was investigated using AFM. Figure 4e shows a flat surface for $Tb_{24}Co_{76}$ in comparison to the other composition. Surface roughness (R_a) for Tb–Co increases with increasing Tb concentration. Therefore, the variation in the exchange bias field as a function of the Tb composition might be related to the interface roughness induced by changes in growth conditions, depending on the Tb content of the alloy.

For the Tb_xCo_{100-x} samples, both H_{ex} and σ_{Pw} reach a maximum value of H_{ex} = 8.75 kOe and σ_{Pw} = 1 (erg/cm^2) at x = 24, which are significantly larger than what was observed in the ordinary AFM/FM and FM/FM systems [17,27,36,44,45].

4. Summary

In summary, we have systematically investigated the perpendicular exchange bias and perpendicular exchange energy (PEE) σ_{Pw} of Tb_xCo_{100-x}/Cu(t_{Cu})/$[Co(0.4)/Pt(2)]_2$ ($20 < x < 30$) heterostructures. We replaced the commonly used AFM pinned layer with the ferrimagnet pinning layer. The interlayer thickness and FIM composition of the Tb–Co layer were optimized to obtain large H_{ex} and σ_{Pw}. The advantage of using amorphous RE-TM alloys as a pinned layer is the tunable magnetic properties that depend strongly on composition. The PEE reached a maximum σ_{Pw} = 1 (erg/cm^2) around x = 24 at.%, at room temperature. In this system, we observed two competing mechanisms—one leading to an increase and the other to a decrease—which corresponds to the effect of Tb content on saturation magnetization and the coercivity of heterostructures. The developed FIM/FM films, with a perpendicular exchange bias and a large PEE, will be greatly beneficial in spintronic applications, such as magneto-optical memory and high areal density recording technology.

Author Contributions: Conceptualization, S.R. and H.A.; investigation, S.R.; writing—original draft preparation, S.R.; writing—review and editing, S.R., S.S., K.T. and H.A. All authors have read and agreed to the published version of the manuscript.

Funding: This research received no external funding. This work was supported by the JSPS KAKENHI (grants 21K14202, and 20H02185).

Institutional Review Board Statement: Not applicable.

Informed Consent Statement: Not applicable.

Data Availability Statement: The data presented in this study are available upon reasonable request from the corresponding author.

Acknowledgments: The authors thank Ahmet Yagmur for his valuable discussions.

Conflicts of Interest: The authors declare no conflict of interest.

References

1. Meiklejohn, W.H.; Bean, C.P. New Magnetic Anisotorpy. *Phys. Rev.* **1957**, *105*, 904. [CrossRef]
2. Schuller, I.K. Exchange bias. *J. Magn. Magn. Mater.* **1999**, *192*, 203–232.
3. March, N.H.; Lambin, P.; Herman, F. Cooperative magnetic properties in single-and two-phase 3d metallic alloys relevant to exchange and magnetocrystalline anisotropy. *J. Magn. Magn. Mater.* **1984**, *44*, 1–19. [CrossRef]
4. Ranjbar, S.; Al-Mahdawi, M.; Oogane, M.; Ando, Y. High-Temperature Magnetic Tunnel Junction Magnetometers Based on L1 0 -PtMn Pinned Layer. *IEEE Sens. Lett.* **2020**, *4*, 5–8. [CrossRef]
5. Fujiwara, K.; Oogane, M.; Yokota, S.; Nishikawa, T.; Naganuma, H.; Ando, Y. Fabrication of magnetic tunnel junctions with a bottom synthetic antiferro-coupled free layers for high sensitive magnetic field sensor devices. *J. Appl. Phys.* **2012**, *111*, 5–8. [CrossRef]
6. Baibich, M.N.; Broto, J.M.; Fert, A.; Van Dau, F.N.; Petroff, F.; Eitenne, P.; Creuzet, G.; Friederich, A.; Chazelas, J. Giant magnetoresistance of (001)Fe/(001)Cr magnetic superlattices. *Phys. Rev. Lett.* **1988**, *61*, 2472–2475. [CrossRef]
7. Ranjbar, R.; Suzuki, K.; Sugihara, A.; Ma, Q.L.; Zhang, X.M.; Miyazaki, T.; Ando, Y.; Mizukami, S. Antiferromagnetic coupling in perpendicularly magnetized cubic and tetragonal Heusler bilayers. *Mater. Lett.* **2015**, *160*, 88–91. [CrossRef]
8. Yuasa, S.; Nagahama, T.; Fukushima, A.; Suzuki, Y.; Ando, K. Giant room-temperature magnetoresistance in single-crystal Fe/MgO/Fe magnetic tunnel junctions. *Nat. Mater.* **2004**, *3*, 868–871. [CrossRef]
9. Almeida, J.M.; Ferreira, R.; Freitas, P.P.; Langer, J.; Ocker, B.; Maass, W. 1f noise in linearized low resistance MgO magnetic tunnel junctions. *J. Appl. Phys.* **2006**, *99*, 08B314. [CrossRef]
10. Choi, S.; Lee, K.J.; Choi, S.; Chongthanaphisut, P.; Bac, S.K.; Lee, S.; Liu, X.; Dobrowolska, M.; Furdyna, J.K. Controllable Exchange Bias Effect in (Ga, Mn) As/(Ga, Mn)(As, P) Bilayers with Non-Collinear Magnetic Anisotropy. *IEEE Trans. Magn.* **2021**, *57*, 2–5. [CrossRef]
11. Suzuki, I.; Hamasaki, Y.; Itoh, M.; Taniyama, T. Controllable exchange bias in Fe/metamagnetic FeRh bilayers. *Appl. Phys. Lett.* **2014**, *105*, 172401. [CrossRef]
12. Sbiaa, R.; Piramanayagam, S.N. Multi-level domain wall memory in constricted magnetic nanowires. *Appl. Phys. A Mater. Sci. Process.* **2014**, *114*, 1347–1351. [CrossRef]
13. Atkinson, D.; Eastwood, D.S.; Bogart, L.K. Controlling domain wall pinning in planar nanowires by selecting domain wall type and its application in a memory concept. *Appl. Phys. Lett.* **2008**, *92*, 22510. [CrossRef]
14. Jung, H.S.; Traistaru, O.; Fujiwara, H. Effect of the kinds of ferromagnetic layers on exchange coupling strength in IrMn / FM films Effect of the kinds of ferromagnetic layers on exchange coupling strength in IrMn Ô FM films. *J. Appl. Phys.* **2004**, *95*, 6849–6851. [CrossRef]
15. Schmid, I.; Marioni, M.A.; Kappenberger, P.; Romer, S.; Parlinska-Wojtan, M.; Hug, H.J.; Hellwig, O.; Carey, M.J.; Fullerton, E.E. Exchange bias and domain evolution at 10 nm scales. *Phys. Rev. Lett.* **2010**, *105*, 197201. [CrossRef]
16. Tsunoda, M.; Nishikawa, K.; Damm, T.; Hashimoto, T.; Takahashi, M. Extra large unidirectional anisotropy constant of Co-Fe/Mn-Ir bilayers with ultra-thin antiferromagnetic layer. *J. Magn. Magn. Mater.* **2002**, *239*, 182–184. [CrossRef]
17. Ranjbar, S.; Tsunoda, M.; Oogane, M.; Ando, Y. Composition Dependence of Exchange Anisotropy in PtxMn1-x/Co70Fe30 Films. *Jpn. J. Appl. Phys.* **2019**, *58*, 043001. [CrossRef]
18. Cao, Y.; Rushforth, A.W.; Sheng, Y.; Zheng, H.; Wang, K. Tuning a Binary Ferromagnet into a Multistate Synapse with Spin–Orbit-Torque-Induced Plasticity. *Adv. Funct. Mater.* **2019**, *29*, 1808104. [CrossRef]
19. Ranjbar, S.; Tsunoda, M.; Al-mahdawi, M.; Oogane, M.; Ando, Y. Compositional Dependence of Exchange Anisotropy in PtxMn100−x/CoyFe100−y Films. *IEEE Magn. Lett.* **2019**, *10*, 1–5. [CrossRef]
20. Mangin, S.; Montaigne, F.; Schuhl, A. Interface domain wall and exchange bias phenomena in ferrimagnetic/ferrimagnetic bilayers. *Phys. Rev. B Condens. Matter Mater. Phys.* **2003**, *68*, 140404. [CrossRef]
21. Hebler, B.; Böttger, S.; Nissen, D.; Abrudan, R.; Radu, F.; Albrecht, M. Influence of the Fe-Co ratio on the exchange coupling in TbFeCo/[Co/Pt] heterostructures. *Phys. Rev. B* **2016**, *93*, 184423. [CrossRef]
22. Tokunaga, T.; Taguchi, M.; Fukami, T.; Nakaki, Y.; Tsutsumi, K. Study of interface wall energy in exchange-coupled double-layer film. *J. Appl. Phys.* **1990**, *67*, 4417–4419. [CrossRef]
23. Lin, C.C.; Lai, C.H.; Jiang, R.F.; Shieh, H.P.D. High interfacial exchange energy in TbFeCo exchange-bias films. *J. Appl. Phys.* **2003**, *93*, 6832–6834. [CrossRef]
24. Romer, S.; Marioni, M.A.; Thorwarth, K.; Joshi, N.R.; Corticelli, C.E.; Hug, H.J.; Oezer, S.; Parlinska-Wojtan, M.; Rohrmann, H. Temperature dependence of large exchange-bias in TbFe-Co/Pt. *Appl. Phys. Lett* **2012**, *101*, 222404. [CrossRef]
25. Radu, F.; Abrudan, R.; Radu, I.; Schmitz, D.; Zabel, H. Perpendicular exchange bias in ferrimagnetic spin valves. *Nat. Commun.* **2012**, *3*, 715. [CrossRef] [PubMed]
26. Hebler, B.; Reinhardt, P.; Katona, G.L.; Hellwig, O.; Albrecht, M. Double exchange bias in ferrimagnetic heterostructures. *Phys. Rev. B* **2017**, *95*, 104410. [CrossRef]
27. Canet, F.; Mangin, S.; Bellouard, C.; Piecuch, M. Positive exchange bias in ferromagnetic-ferrimagnetic bilayers: FeSn/FeGd. *Europhys. Lett.* **2000**, *52*, 594–600. [CrossRef]
28. Finley, J.; Liu, L. Spin-Orbit-Torque Efficiency in Compensated Ferrimagnetic Cobalt-Terbium Alloys. *Phys. Rev. Appl.* **2016**, *6*, 054001. [CrossRef]

29. Gottwald, M.; Hehn, M.; Montaigne, F.; Lacour, D.; Lengaigne, G.; Suire, S.; Mangin, S. Magnetoresistive effects in perpendicularly magnetized Tb-Co alloy based thin films and spin valves. *J. Appl. Phys.* **2012**, *111*, 083904. [CrossRef]
30. Siddiqui, S.A.; Han, J.; Finley, J.T.; Ross, C.A.; Liu, L. Current-Induced Domain Wall Motion in a Compensated Ferrimagnet. *Phys. Rev. Lett.* **2018**, *121*, 57701. [CrossRef]
31. Schubert, C.; Hebler, B.; Schletter, H.; Liebig, A.; Daniel, M.; Abrudan, R.; Radu, F.; Albrecht, M. Interfacial exchange coupling in Fe-Tb/[Co/Pt] heterostructures. *Phys. Rev. B Condens. Matter Mater. Phys.* **2013**, *87*, 054415. [CrossRef]
32. Shimanuki, S.; Ichihara, K.; Yasuda, N.; Ito, K.; Kohn, K. Magnetic and Magneto-Optical Properties of Amorphous TbCo Films Prepared by Two Target Magnetron Co-sputtering. *J. Magn. Soc. Jpn.* **1986**, *10*, 179–182. [CrossRef]
33. Tang, M.; Zhang, Z.; Jin, Q. Manipulation of perpendicular exchange bias effect in [Co/Ni]N/(Cu, Ta)/TbCo multilayer structures. *AIP Adv.* **2015**, *5*, 087153. [CrossRef]
34. Joo, S.J.; Hong, D.H.; Lee, T.D. Effect of Cu inserted layer between the IrMn and CoFeB interface on magnetic properties of CoFeB. *J. Appl. Phys.* **2004**, *95*, 7522–7524. [CrossRef]
35. Sheng, Y.; Edmonds, K.W.; Ma, X.; Zheng, H.; Wang, K. Adjustable Current-Induced Magnetization Switching Utilizing Interlayer Exchange Coupling. *Adv. Electron. Mater.* **2018**, *4*, 1800224. [CrossRef]
36. Tang, M.; Zhao, B.; Zhu, W.; Zhu, Z.; Jin, Q.Y.; Zhang, Z. Controllable Interfacial Coupling Effects on the Magnetic Dynamic Properties of Perpendicular [Co/Ni] 5 /Cu/TbCo Composite Thin Films. *ACS Appl. Mater. Interfaces* **2018**, *10*, 5090–5098. [CrossRef]
37. Tang, M.H.; Zhang, Z.; Tian, S.Y.; Wang, J.; Ma, B.; Jin, Q.Y. Interfacial exchange coupling and magnetization reversal in perpendicular [Co/Ni]N/TbCo composite structures. *Sci. Rep.* **2015**, *5*, 10863. [CrossRef]
38. Hansen, P.; Klahn, S.; Clausen, C.; Much, G.; Witter, K. Magnetic and magneto-optical properties of rare-earth transition-metal alloys containing Dy, Ho, Fe, Co. *J. Appl. Phys.* **1991**, *69*, 3194–3207. [CrossRef]
39. Harres, A.; Geshev, J. A polycrystalline model for magnetic exchange bias. *J. Phys. Condens. Matter* **2012**, *24*, 326004. [CrossRef]
40. Alebrand, S.; Gottwald, M.; Hehn, M.; Steil, D.; Cinchetti, M.; Lacour, D.; Fullerton, E.E.; Aeschlimann, M.; Mangin, S. Light-induced magnetization reversal of high-anisotropy TbCo alloy films. *Appl. Phys. Lett.* **2012**, *101*, 162408. [CrossRef]
41. Baruth, A.; Keavney, D.J.; Burton, J.D.; Janicka, K.; Tsymbal, E.Y.; Yuan, L.; Liou, S.H.; Adenwalla, S. Origin of the interlayer exchange coupling in [Co/Pt]/NiO/[Co/Pt] multilayers studied with XAS, XMCD, and micromagnetic modeling. *Phys. Rev. B* **2006**, *74*, 054419. [CrossRef]
42. Lederman, D.; Nogués, J.; Schuller, I.K. Exchange anisotropy and the antiferromagnetic surface order parameter. *Phys. Rev. B Condens. Matter Mater. Phys.* **1997**, *56*, 2332–2335. [CrossRef]
43. Kumar, D.; Singh, S.; Gupta, A. Effect of interface roughness on exchange coupling in polycrystalline Co/CoO bilayer structure: An in-situ investigation. *J. Appl. Phys.* **2016**, *120*, 085307. [CrossRef]
44. Hauet, T.; Mangin, S.; McCord, J.; Montaigne, F.; Fullerton, E.E. Exchange-bias training effect in TbFe GdFe: Micromagnetic mechanism. *Phys. Rev. B Condens. Matter Mater. Phys.* **2007**, *76*, 144423. [CrossRef]
45. Tsunoda, M.; Yoshitaki, S.; Ashizawa, Y.; Kim, D.Y.; Mitsumata, C.; Takahashi, M. Enhancement of exchange bias by ultra-thin Mn layer insertion at the interface of Mn-Ir/Co-Fe bilayers. *Phys. Status Solidi Basic Res.* **2007**, *244*, 4470–4473. [CrossRef]